Journal of Applied Physics ARTICLE pubs.aip.org/aip/jap

Dangling bonds, the charge neutrality level, and band alignment in semiconductors

Cite as: J. Appl. Phys. **135**, 075703 (2024); doi: 10.1063/5.0190043
Submitted: 2 December 2023 · Accepted: 24 January 2024 ·
Published Online: 16 February 2024

View Online Export Citation CrossMark

J. B. Varley,[1,2,a)] J. R. Weber,[3] A. Janotti,[4] and C. G. Van de Walle[5]

AFFILIATIONS

[1]Materials Science Division, Lawrence Livermore National Laboratory, 7000 East Ave, Livermore, California 94550, USA
[2]Laboratory for Energy Applications for the Future, Lawrence Livermore National Laboratory, 7000 East Ave, Livermore, California 94550, USA
[3]Logic Technology Division, Intel Corporation, Hillsboro, Oregon 97124, USA
[4]Department of Materials Science and Engineering, University of Delaware, Newark, Delaware 19716, USA
[5]Materials Department, University of California, Santa Barbara, California 93106-5050, USA

Note: This paper is part of the Special Topic on Native Defects, Impurities and the Electronic Structure of Compound Semiconductors: A Tribute to Dr. Wladyslaw Walukiewicz.

[a)]**Author to whom correspondence should be addressed:** varley2@llnl.gov

ABSTRACT

We present a systematic study of the electronic properties of dangling bonds (DBs) in a variety of semiconductors and examine the relationship between DBs and the charge neutrality level (CNL) in the context of band alignments of semiconductors. We use first-principles calculations based on density functional theory to assess the energetics of DBs in a set of diamond-structure group-IV and III–V or II–VI zinc-blende-structure semiconductors, considering both cation and anion-derived states. We examine the charge-state transition levels of DBs to assess whether they can serve as a CNL to align band structures, by comparing with offsets calculated from interface calculations. Our results show that this approach for evaluating the CNL yields quantitative results for band offsets and provides useful insights. We discuss the relation with alternative approaches for determination of CNLs based on branch-point energies or transition levels of interstitial hydrogen.

I. INTRODUCTION:

Understanding the properties of dangling bonds (DBs) in semiconductors is crucial for understanding interfaces, surfaces, and point defects such as vacancies. Conceptually, DBs are readily associated with sp^3 hybrid orbitals in tetrahedrally bonded semiconductors; in practice, however, explicit calculations for DBs are challenging because realistic DBs at surfaces or interfaces can occur in an array of different configurations, rendering it difficult to extract generic properties. In a point defect such as a vacancy, DBs tend to interact strongly with one another, making it difficult to extract information about individual DBs. We overcome this obstacle by modeling an isolated DB by creating a small void inside the material and passivating all but one of the resulting DBs with hydrogen (see Fig. 1).[1]

In the present work, we use this geometry to perform a systematic study of isolated DBs in group-IV, III–V, and II–VI semiconductors. The results allow us to investigate trends in the electronic properties of the dangling bonds, such as the dependence on lattice constant and atomic sizes of the host atoms. We specifically examine the relationship between DBs and band alignments. It has been suggested that DB energies can be used to predict semiconductor band alignments.[2–4] This has been explained by invoking the concept of the charge neutrality level (CNL),[4–9] which represents an effective energy level where the bulk states change from a predominantly valence-band-like or donor-like character to conduction-band-like or acceptor-like character. The original concept derives from virtual or metal-induced gap states in the context of Schottky barriers and has had considerable success in describing observed Fermi-level pinning in metal–semiconductor

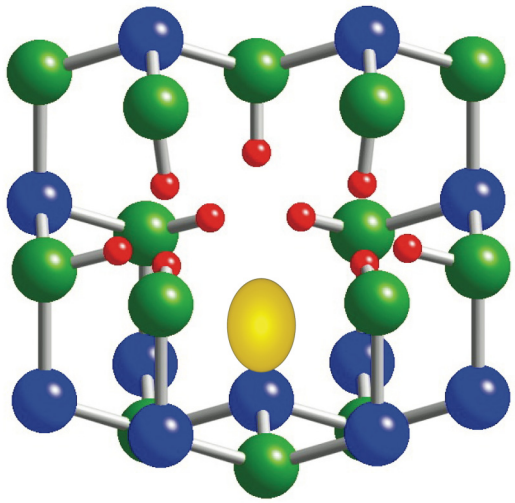

FIG. 1. DB geometry for a cation DB in a zinc-blende semiconductor. Large blue atoms indicate cations, and green atoms indicate anions in a compound (III–V or II–VI) semiconductor. In diamond-structure group-IV semiconductors, the host atoms are all of one type. The isolated DB is indicated by the gold oval. The small red atoms indicate pseudohydrogen atoms used to passivate the remaining DBs.

contacts.[5,10] The CNL was subsequently invoked for establishing a common reference level on which to align the unstrained or "natural" band edges of semiconductors and insulators.[4,6,7,9,11–17] Seminal work by Walukiewicz also made the connection with point defects[3,18,19] as well as with doping trends.[19,20]

These studies explored various quantities that can be used to determine the CNL, for instance, the branch-point energy (E_{BP}),[5,9,10,12,14,16,21–23] the dielectric midgap energy (E_{DME}),[15,24] or the charge-state transition level associated with interstitial hydrogen, H_i $(+/-)$.[4,8] The connection between E_{BP}, ionization potentials (IPs), and interfacial band offsets was explored by Hinuma *et al.*,[16] who found that E_{BP}-based alignments could predict calculated average interfacial offsets within ~ 0.1 eV. The connection between band alignments and DBs was explored within the tight-binding theory by Tersoff and Harrison,[6,7] and for a small number of III–V compounds by Komsa and Pasquarello.[25] In Ref. 17, several individual formulations of the CNL such as the E_{BP}, E_{DME} and H_i $(+/-)$ were systematically evaluated in III–V and II–V compounds and compared with the defect levels associated with cation vacancies that result from the hybridization of anion-related DBs. However, the link between cation and anion-derived DBs and alternative definitions of the CNL remains unclear.

Here, we systematically explore the average energy of DB charge-state transition levels and the connection to the CNL by performing first-principles calculations of model DBs for a set of group-IV, III–V, and II–VI semiconductors. We examine trends in the electronic properties of the DBs and compare the results for the DB-derived CNLs with band alignments previously obtained from the explicit interface or natural band-offset calculations, as well as from other CNL-based approaches. We find that the DB-derived levels are in remarkable agreement with branch-point energies. They also show the same trend as CNLs based on the transition level of interstitial hydrogen, except for a systematic shift that we can attribute to the fact that different charge states of the DB are being probed.

II. COMPUTATIONAL APPROACH

A. Modeling a dangling bond

In our calculations, we utilize a geometry that enables us to study isolated DBs in a variety of semiconductors. Figure 1 illustrates this geometry for a cation DB in a zinc-blende-structure compound such as a III–V material. The DB structure is created by making a small void inside the crystal, specifically by removing four atoms.[1] We first remove an anion; this creates a vacancy with four strongly interacting cation DBs. Then, we remove three of the cation atoms that neighbor the vacancy, resulting in nine new anion DBs, far removed from the original cation DB. These nine new DBs can then be passivated with pseudohydrogen atoms. Electron counting tells us that a group-V anion contributes 5/4 of an electron to each of the four bonds around it; so, the anion DB can be passivated by attaching a pseudohydrogen atom with a valence of 3/4. This leaves behind a single isolated cation DB.

The anion-H bonds contribute to the total energy of the entire structure. However, our goal in the present work is not to find a formation energy for the DB but to focus on the *differences* in formation energy that determine charge-state transition levels. The anion-H bond distances are optimized through structural relaxations; we do this for a "fully passivated" neutral structure, i.e., a structure in which the DB is also passivated by (pseudo)hydrogen (with an appropriate valence; see below). When calculating structures and energies for the positive, neutral, and negative charge states of the DB, we start from the geometry determined as specified above and include atomic relaxations up to second-nearest neighbors of the atom on which the DB resides. Contributions from further shells of atoms, including the anion-H bonds, thus cancel in the energy differences that determine charge-state transition levels.

Studying an anion DB would simply require interchanging the (blue) cations and (green) anions in Fig. 1; the red pseudohydrogen atoms now passivate cations and hence need a valence of 5/4. For a II–VI material, the pseudohydrogens would need valence 1/2 to passivate anion DBs and valence 3/2 to passivate cation DBs. In a group-IV material, finally, the two types of atoms in the unit cell are identical, leading to the diamond structure, in which dangling bonds can be passivated with "regular" hydrogen with valence 1.

By calculating the formation energy (as defined in Ref. 26) for the DB occupied with zero, one, and two electrons, we can calculate the thermodynamic charge-state transition levels associated with the DB. This procedure has been previously used to study DBs in silicon,[1,27,28] germanium,[28,29] SiGe alloys,[30] III-arsenides,[25] and Al_2O_3.[31,32]

For a DB in a group-IV material, occupying the DB with zero, one, or two electrons leads to a net charge on the supercell of $+1$, 0, or -1. Charged supercells are treated in the usual approach that corrects for spurious interactions.[26,33] For a cation DB in a III–V

compound, the net charges in the supercell are +0.75, −0.25, and −1.25 for the unoccupied (zero electrons), partially occupied (one electron), and fully occupied (two electrons) defect states, i.e., the "donor," "neutral," and "acceptor" configurations of the DB. The corresponding net charges for an anion DB are +1.25, +0.25, and −0.75. In a II–VI compound, the corresponding net charges are +0.5, −0.5, and −1.5 for the cation DB and +1.5, +0.5, and −0.5 for the anion DB. Spin polarization was included for all calculations involving unpaired electrons.

B. Density functional calculations

The calculations presented here are based on a generalized Kohn–Sham scheme, utilizing the HSE06 screened hybrid functional[34] and projector-augmented wave (PAW) approach[35] as implemented in the VASP code.[36,37] Indium 4*d* electrons were explicitly included as valence states in all cases. Ga 3*d* electrons were included explicitly only in the case of GaN, as in prior work.[17] Semicore *d* states are always included as valence states for the group-II atoms. The fraction of non-local Hartree–Fock exchange (α) included in the HSE06 functional was adjusted for each material to match the experimental bandgaps (taking spin–orbit splitting into account, see below) and is listed in Table I.

All bulk unit cell calculations were optimized using two-atom primitive unit cells of the zinc-blende and diamond lattices to identify the optimal lattice constants and resulting properties for each chosen α value. The energy cutoff in the plane wave expansion is chosen to be 400 eV. Spin–orbit effects were not explicitly considered in the defect calculations but added as a post-correction to the valence-band position from the calculated spin–orbit splitting. The calculated spin–orbit splittings (Δ_{SO}) are included in Table I as taken from Ref. 17; corrections to the valence-band maximum are included as $+\Delta_{SO}/3$ and accounted for in the quoted bandgap values.

For the DB calculations, we used supercells that are 2 × 2 × 2, 3 × 3 × 3, or 4 × 4 × 4 multiples of the conventional zinc-blende

TABLE I. Summary of diamond and zinc-blende materials studied, showing the used fraction of HF exact exchange (α), the resulting bandgap accounting for spin–orbit effects (E_g), the calculated spin–orbit splitting (Δ_{SO}), the lattice constant *a*, the low-frequency dielectric constant used in the finite-size corrections ε, the final computed transition levels for the anion DBs and the cation DBs and their corresponding *U* values as described in the text. All values are referenced to the VBM of each material. We also list the DB charge-neutrality levels (CNLs) calculated in the present work from the average DB energies (E_{DB}), along with branch-point energies (E_{BP}), and (+/ −) transition levels of interstitial H (H_i) taken from Ref. 17.

	α	E_g	Δ_{SO}	a	ε	Anion DB (eV)			Cation DB (eV)				Charge neutrality levels (eV)			
	(%)	(eV)	(eV)	(Å)	(ε_0)	(+/0)	(+/ −)	(0/ −)	U_A	(+/0)	(+/ −)	(0/ −)	U_C	E_{DB}	E_{BP}	H_i (+/ −)
C	25	5.31	0.01	3.55	5.7	−0.33	0.78	1.88	2.20	−0.33	0.78	1.88	2.20	0.78	1.45	2.57
Si	25	1.17	0.00	5.44	12.1	0.05	0.44	0.82	0.78	0.05	0.44	0.82	0.78	0.44	0.14	0.74
Ge	32	0.81	0.32	5.68	16.1	−0.29	−0.11	0.07	0.35	−0.29	−0.11	0.07	0.35	−0.11	−0.23	0.39
SiC	32	2.50	0.02	4.34	9.5	−0.05	1.01	2.07	2.12	1.42	2.01	2.61	1.19	1.51	2.07	1.87
SiGe	32	1.19	0.19	5.55	13.9	−0.08	0.19	0.46	0.54	−0.13	0.23	0.59	0.72	0.21	0.01	−0.06
BN	32	6.20	0.02	3.59	6.9	−1.16	0.23	1.63	2.79	2.82	3.75	4.69	1.87	1.99	3.52	4.13
BP	32	2.16	0.05	4.51	9.3	−0.55	−0.11	0.34	0.89	0.56	1.33	2.10	1.53	0.61	0.66	1.12
BAs	25	1.75	0.20	4.78	9.9	−0.49	−0.28	−0.07	0.42	0.23	0.96	1.69	1.46	0.34	0.33	0.69
BSb	25	1.06	0.37	5.24	12.0	−0.53	−0.43	−0.32	0.21	−0.17	0.49	1.15	1.33	0.03	0.03	0.31
AlN	32	4.92	0.02	4.36	8.6	−0.49	1.22	2.92	3.41	3.57	4.35	5.13	1.56	2.79	3.10	3.36
AlP	32	2.47	0.07	5.46	9.8	−0.51	0.19	0.89	1.40	1.96	2.35	2.73	0.77	1.27	1.38	1.48
AlAs	32	2.16	0.32	5.68	10.1	−0.55	−0.01	0.53	1.08	1.53	1.83	2.13	0.60	0.91	0.96	1.05
AlSb	32	1.63	0.70	6.18	12.0	−0.63	−0.29	0.04	0.68	0.82	1.03	1.24	0.41	0.37	0.40	0.51
GaN	32	3.52	0.00	4.53	10.1	−1.23	0.34	1.91	3.14	2.45	2.89	3.33	0.89	1.62	2.13	2.92
GaP	32	2.47	0.10	5.47	11.1	−0.68	−0.14	0.41	1.08	1.39	1.53	1.66	0.27	0.70	0.84	1.42
GaAs	32	1.46	0.37	5.68	12.9	−0.66	−0.32	0.02	0.68	1.00	1.02	1.04	0.04	0.35	0.43	0.91
GaSb	32	0.77	0.76	6.14	15.7	−0.84	−0.58	−0.33	0.51	0.44	0.40	0.37	−0.07	−0.09	−0.08	0.28
InN	32	0.86	0.00	5.04	15.3	−1.05	0.37	1.79	2.84	1.84	2.03	2.22	0.38	1.20	1.35	2.12
InP	32	1.66	0.12	5.93	12.4	−0.70	−0.07	0.56	1.27	1.43	1.49	1.56	0.13	0.71	0.77	1.39
InAs	32	0.53	0.39	6.12	14.6	−0.74	−0.29	0.17	0.90	1.07	1.04	1.01	−0.06	0.38	0.42	0.95
InSb	32	0.28	0.80	6.56	16.8	−0.77	−0.49	−0.21	0.56	0.59	0.50	0.41	−0.18	0.01	0.04	0.45
CdS	32	2.42	0.07	5.89	9.6	−0.86	−0.14	0.57	1.43	2.97	3.00	3.03	0.06	1.43	1.73	2.33
CdSe	36	1.83	0.42	6.14	9.2	−0.88	−0.25	0.38	1.25	2.62	2.59	2.56	−0.06	1.17	1.40	1.88
CdTe	36	1.61	0.94	6.56	10.2	−1.04	−0.56	−0.09	0.95	1.96	1.83	1.70	−0.27	0.63	0.91	1.23
ZnS	36	3.83	0.08	5.42	8.2	−0.85	−0.13	0.60	1.45	3.46	3.49	3.52	0.06	1.68	2.04	2.53
ZnSe	36	2.73	0.45	5.70	8.6	−0.87	−0.31	0.25	1.13	2.86	2.81	2.75	−0.11	1.25	1.52	1.91
ZnTe	36	2.27	0.98	6.15	10.3	−1.08	−0.67	−0.26	0.83	2.04	1.99	1.95	−0.09	0.66	0.87	1.04

or diamond eight-atom unit cells, and thus consist of 64, 216, or 512 atoms. Integrations over the Brillouin zone used a $2 \times 2 \times 2$ mesh of Monkhorst–Pack k-points for the 64-atom cells, and a single off-Γ point at $k = [0.25, 0.25, 0.25]$ for the 216- and 512-atom cells. Comparisons of results for different supercell sizes allowed us to ensure that the reported charge-state transition levels are converged to ~ 0.1 eV or less even with 64-atom supercells, except for cases such as the compounds containing boron and carbon, and some of the nitrides, that exhibit the smallest bond-lengths of the materials studied. For example, for diamond, we find the results for 64-atom (216-atom) supercells to be converged to within 0.17 (0.05 eV). The reported transition levels for larger lattice-constant materials (the II–VI materials, GaSb, InP, InAs, and InSb) are for 64-atom supercells, while all others correspond to 216-atom supercells. Our comparison to results for E_{BP} and the H_i $(+/-)$ is based on previously reported calculations that are described in detail in Ref. 17.

C. Formation energies, charge-state transition levels, and the CNL

To derive the charge-state transition levels associated with the DBs, we calculate the defect formation energies (E^f) for the unoccupied, half-occupied, and fully occupied DB levels using the standard supercell approach.[26] For example, following this approach, the formation energy of a DB defect in Si is given by

$$E^f[\mathrm{DB}^q] = E_{\mathrm{tot}}[\mathrm{DB}^q] - E_{\mathrm{tot}}[\mathrm{DB:H}] + \mu_{\mathrm{H}} + q(\varepsilon_F + \varepsilon_v) + \Delta^q. \quad (1)$$

Here, $E_{\mathrm{tot}}[\mathrm{DB}^q]$ is the total energy of the supercell containing the Si DB in charge state q (i.e., a supercell with 9 H atoms), while $E_{\mathrm{tot}}[\mathrm{DB:H}]$ is the total energy of the reference structure in which the DB is passivated with hydrogen (i.e., a supercell with 10 H atoms). μ_{H} denotes the chemical potential of hydrogen. ε_F is the Fermi level, which is referenced to the energy of the valence-band maximum (VBM) ε_v. Δ^q is a correction term that account for finite-size effects in charged supercells, determined within the scheme of Freysoldt *et al.*[33] and adopting the static dielectric constants summarized in Refs. 17 and 38.

In Fig. 2, we plot the formation energies as a function of Fermi level for the $+1$, 0, and -1 charge states of the DB in Si and for the $+1$, 0, and -1 charge states of the Si and C DBs in SiC. In this work, we do not use the actual values of formation energies but focus on charge-state transition levels, which are defined as the Fermi-level positions where the most favorable charge state changes from $+1$ to 0 or 0 to -1 and thus correspond to crossing points of the formation-energy lines. In Fig. 2(a), the intersection of the formation energy of the unoccupied donor $(+1)$ and partially-occupied neutral (0) states occurs at 0.05 eV above the VBM (as discussed extensively in Ref. 30) and is denoted by the $(+/0)$ charge-state transition level. The $(0/-)$ charge-state transition level is seen to occur at 0.82 eV above the VBM. The CNL can be associated with[4–6,8,21,39] the average of the $(+/0)$ and $(0/-)$ charge-state transition levels, which we denote as E_{DB}; it is easily seen that this average corresponds to the $(+/-)$ transition level, at 0.43 eV above the Si VBM.

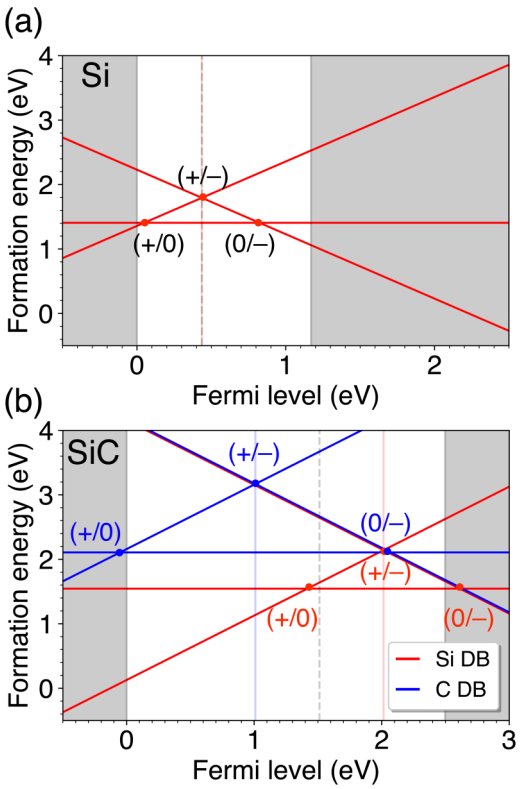

FIG. 2. Formation energy of the Si DB in the $+1$, 0, and -1 charge states, shown as a function of the Fermi level. The hydrogen chemical potential was chosen as half the energy of an H_2 molecule. Regions below the VBM and above the CBM are shaded gray, and the energy corresponding to the transition between the donor- and acceptor-like states is marked with a vertical red line, denoting our definition of the CNL. (b) Analogous plot for Si and C DBs in SiC. We again use a red vertical line to highlight the energies corresponding to the transition between the donor and acceptor states for the Si DB, and a vertical blue line for the C DB. Finally, the average energy of the anion and cation DBs (the red and blue lines) that represents a value for the CNL is marked with a dashed black line.

In Fig. 2(b), we depict the corresponding energies for DBs in a compound material. We choose SiC since this avoids the complications associated with charge states for DBs in III–V or II–VI materials discussed in Sec. II A but still illustrates the presence of two different types of DBs. For SiC, we report results for both Si and C DBs, corresponding to the cation and anion DBs in a compound material. The $(+/-)$ transition level for each type of DB can be determined, falling at 1.01 and 2.01 eV above the SiC VBM for C and Si DBs, respectively. In the compound materials, we will associate the CNL with the average of the $(+/-)$ transition levels for each type of DB; in SiC, this results in an average DB energy at 1.51 eV, which we denote as E_{DB} and summarize in Table I.

We note that in Fig. 2, the $(0/-)$ level occurs at a higher (Fermi-level) energy than the $(+/0)$ transition level. This is what one intuitively expects: the additional electron added to a neutral dangling bond experiences Coulomb repulsion, thus raising the

energy. The DB is positively charged for a Fermi level below (+/0), neutral for a Fermi level between (+/0) and (0/−), and negatively charged for a Fermi level above (0/−). This ordering of the transition levels corresponds to a "positive-*U*" situation, where *U* represents the Coulomb energy. The value of *U* can be defined as the difference in energy between the (0/−) and the (+/0) transition levels.

In some materials, the DB behaves as a "negative-*U*" center,[40] i.e., the (0/−) transition level lies below the (+/0) level. This may occur when a large difference in lattice relaxation occurs for differently occupied states of the DB. In a negative-*U* system, the neutral DB (occupied with one electron) is not thermodynamically stable for any value of the Fermi level, and the only thermodynamically relevant transition is (+/−). Negative-*U* systems occur in other semiconductor defects, such as interstitial hydrogen[4,8] and oxygen vacancies,[41,42] both of which are strongly connected with the behavior of cation DBs. Another class of related defects are *DX*-centers, or donor defects that can undergo large lattice distortions to convert into compensating acceptors that can also exhibit significant character from cation-related DB states.[43–46] Examples will be discussed in Sec. III A. Finally, we note that regardless of positive-*U* or negative-*U* character, the relevant transition for determining the average DB level is the (+/−) level.

The exact same procedure can be followed for cation and anion DBs in the III–V and II–VI compounds. The definition of formation energy, Eq. (1), is easily adapted to this case; the formation energies of individual charge states depend on the chemical potential of pseudohydrogen, but this value cancels in the calculation of charge-state transition levels. As discussed above for SiC, for compound semiconductors, the CNL is defined as the average of the (+/−) levels obtained separately for the cation DB and the anion DB. For instance, in GaAs (see Table I), the (+/−) level occurs at −0.32 eV above the VBM for the As DB and at 1.02 eV for the Ga DB, leading to a E_{DB} CNL at 0.35 eV above the GaAs VBM.

This example illustrates that charge-state transition levels can occur outside the bandgap, i.e., as resonances in the valence band or conduction band. Such a situation indicates that a particular charge state of the DB would not be thermodynamically stable, but as long as we can perform a calculation for that charge state (i.e., identify a locally stable structure), it poses no problem for the formalism.

III. RESULTS AND DISCUSSION

A. DB levels and trends

We have performed this procedure for DBs in group-IV elemental semiconductors (diamond, silicon, and germanium), SiC, SiGe, and various III–V and II–VI zinc-blende semiconductors; the results are summarized in Table I. The results agree well (within 0.2 eV) with the limited number of previously reported values.[1,25,27–31]

Table I shows that in the majority of materials, the DBs behave as positive-*U* centers (see Sec. II C). However, a number of cation DBs, such as Ga DBs in GaSb (and *nearly* GaAs) and In DBs in InAs and InSb, form negative-*U* systems,[40] i.e., with the (+/0) transition level occurring above the (0/−) transition level. Similarly, in the II–VIs, Cd and Zn DBs are negative-*U* or exhibit very small positive *U* values.

The values of *U* also behave systematically. The value of *U* generally decreases as the lattice constant increases. e.g., among the studied group-IV semiconductors, Ge has the largest lattice constant, and the Ge DB has the smallest *U* value. For the compound semiconductors, *U* values are larger for anion DBs than for cation DBs. Both of these trends can be understood based on the relation of *U* to electron localization and structural relaxation.[40] As the lattice constant decreases, the material becomes more rigid, thus inhibiting structural relaxation upon the addition (removal) of electrons to (from) a DB. In addition, anion DBs tend to be more spatially localized than cation DBs. Adding a second electron to an anion DB will, therefore, require more energy than for a cation DB in the same material, leading to a larger value of *U*.

The anion vs cation DB trend does not hold in a few select cases, such as BP, BAs, BSb, and SiGe. These happen to be materials in which the cation size is smaller than the anion size (based on, e.g., their covalent radii[47]), and hence the spatial localization argument is reversed.

B. Consequences for materials and devices

In Si, all transition levels associated with the DB occur within the bandgap. This explains (at least in part) why hydrogen passivation of DBs at the Si/SiO_2 interface is so successful. Without such passivation, the Si DBs could trap electrons, thus interfering with device performance and leading to degradation. Since interstitial hydrogen in Si is also amphoteric (meaning it can act both as a donor and an acceptor), it is always feasible to form a Si–H bond, thus passivating the Si DB.

Some other materials produce DBs with levels that occur either below the VBM or above the CBM. For example, in Ge, all DB transition levels occur below the VBM.[29] This means that, regardless of doping, germanium DBs will always be negatively charged. Because hydrogen is also exclusively negatively charged (the correlation between the electronic behaviors of interstitial H and of the DB is not incidental—see Ref. 4), H will be repelled from DBs and passivation will be inhibited.

Similarly, in InN, the indium DB produces transition levels above the CBM, causing the indium DB to be always positively charged. Combined with the fact that hydrogen acts exclusively as a donor in InN,[48] we conclude that In DBs in InN will be difficult to passivate.

The information we present here on DB levels produces useful insights into other cases as well. For example, BAs, recently championed as a near-ideal semiconductor showing high dopability combined with excellent thermal and ambipolar electronic conductivity,[49–51] has exclusively negatively charged As DBs (similar to Ge), while B DBs possess transitions within the bandgap, similar to Si and cations in AlAs and GaAs.[25] However, in contrast to cations in the other III-arsenides, the B DB is predominantly stable in the neutral charge state (nearly never stable in the negative charge state) and is hence less likely to repel H_i, which has a calculated (+/−) level 0.7 eV above the BAs VBM.[17] This suggests DB passivation at BAs-oxide interfaces may be easier as compared to other III-As compounds.[25,52]

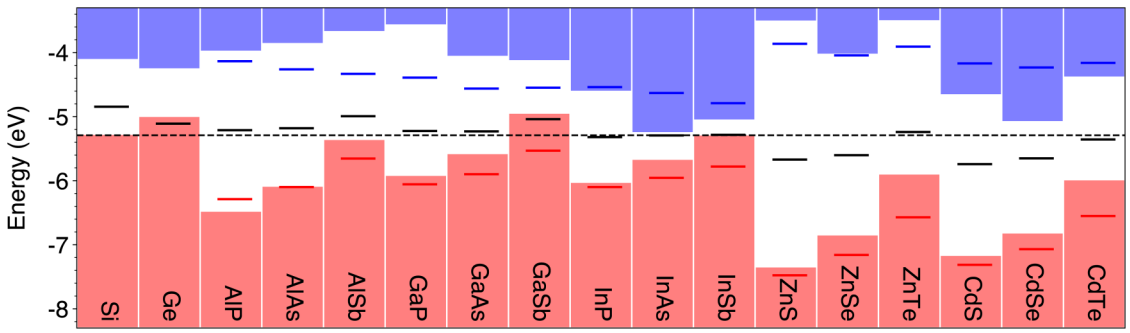

FIG. 3. Average DB levels (E_{DB}) in select group-IV, III–V, and II–VI semiconductors, aligned on an absolute energy scale. Valence-band (red) and conduction-band (blue) edges are aligned based on the natural band offsets reported in Ref. 16 and summarized in Table II. Alignment with the vacuum level is achieved by placing the Si conduction band at 4.11 eV below the vacuum level (corresponding to the Si electron affinity) from Ref. 16 for the (111) 2×1 Si surface. In the elemental semiconductors (Si and Ge), there is only one type of DB; in the compound semiconductors, we report values for the cation DB (blue) and for the anion DB (red), with the average of those (black) providing the average DB level E_{DB}, which we identify with the CNL. The dashed black line reflects the average of the E_{DB} on an absolute energy scale of -5.29 ± 0.24 eV assuming these band alignments, as described in the text.

C. Band alignment

We have used our results for the $(+/-)$ levels of cation and anion DBs (Table I) to calculate E_{DB} for each material, defined as the average of the $(+/-)$ levels for the anion and cation DBs. To get insight into where these levels lie on an absolute energy scale, we compare their positions by plotting them referenced to the VBM in each material and aligning these VBM values using reported band-offset values. In Fig. 3, the valence and conduction bands have been aligned on an absolute energy scale using the natural band offsets reported by Hinuma *et al.*[16] based on explicit interface calculations with hybrid functionals and additional corrections from many-body perturbation theory. To align with the vacuum level, we used the Si electron affinity (EA), which places the Si conduction-band minimum at 4.11 eV below the vacuum level as calculated by Hinuma *et al.*[16] for the (111) (2×1) Si surface. The offsets from Ref. 16 are summarized in Table II. The table also contains our calculated E_{DB} values, and two other possible ways of defining the CNL: the branch-point energy and H_i

TABLE II. Experimental bandgaps[38] and calculated valence- and conduction-band offsets (VBO, CBO) assuming an alignment to Si using the calculated band offsets reported by Hinuma *et al.*[16] and by Van de Walle and Neugebauer.[4] We also list the offsets associated with the various charge-neutrality levels (CNLs) summarized in Table I as also aligned to Si, for the average DB energies (E_{DB}), the branch-point energies (E_{BP}), and (+/ −) transition levels of interstitial H taken from Ref. 17. All values are in eV.

		Reference 16		Reference 4		E_{DB}		E_{BP}		H_i (+/ −)	
	E_g (exp)	VBO	CBO	VBO	CBO	VBO	CBO	VBO	CBO	VBO	CBO
Si	1.17	0.00	0.00	0.00	0.00	0.00	0.00	0.00	0.00	0.00	0.00
Ge	0.74	0.28	−0.23	0.58	0.15	0.54	0.18	0.37	0.01	0.35	−0.01
AlP	2.51	−1.20	0.17	−1.40	−0.06	−0.83	0.47	−1.24	0.06	−0.74	0.56
AlAs	2.23	−0.81	0.29	−0.71	0.35	−0.47	0.52	−0.82	0.17	−0.31	0.68
AlSb	1.70	−0.08	0.41	0.25	0.78	0.07	0.53	−0.26	0.20	0.23	0.69
GaP	2.35	−0.64	0.53	−0.68	0.50	−0.26	1.04	−0.70	0.60	−0.68	0.62
GaAs	1.52	−0.30	−0.11	−0.12	0.23	0.09	0.38	−0.29	0.01	−0.17	0.13
GaSb	0.75	0.33	−0.22	0.57	0.15	0.52	0.13	0.23	−0.17	0.46	0.07
InP	1.42	−0.75	−0.52	−0.31	−0.06	−0.28	0.21	−0.63	−0.14	−0.65	−0.16
InAs	0.41	−0.39	−1.25	0.15	−0.61	0.06	−0.59	−0.28	−0.92	−0.21	−0.85
InSb	0.24	−0.01	−1.03	0.67	−0.26	0.43	−0.46	0.10	−0.78	0.29	−0.60
ZnS	3.84	−2.07	0.48	−1.69	0.98	−1.24	1.42	−1.89	0.77	−1.79	0.87
ZnSe	2.83	−1.57	0.01	−1.11	0.55	−0.81	0.75	−1.38	0.18	−1.17	0.39
ZnTe	2.39	−0.62	0.44	−0.18	1.04	−0.23	0.88	−0.72	0.38	−0.30	0.80
CdS	2.50	−1.89	−0.65	−1.37	−0.04	−0.99	0.26	−1.59	−0.34	−1.59	−0.34
CdSe	1.90	−1.54	−0.98	−0.89	−0.16	−0.73	−0.07	−1.26	−0.60	−1.14	−0.48
CdTe	1.59	−0.71	−0.37	−0.27	0.15	−0.20	0.24	−0.76	−0.32	−0.49	−0.05

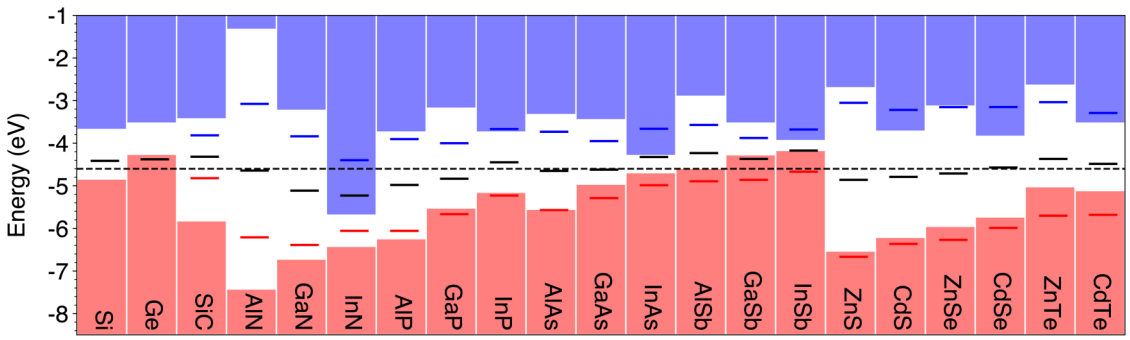

FIG. 4. Average DB levels (E_{DB}) in select group-IV, III–V, and II–VI semiconductors, aligned on an absolute energy scale as in Fig. 3, but with the band edges aligned based on offsets reported in Ref. 4 and also listed in Table II. Alignment with the vacuum level is achieved by placing the Si conduction band at 3.68 eV below the vacuum level (as assumed in Ref. 4). Other details are as in Fig. 3, where the horizontal black lines indicate the average E_{DB} levels defining the CNL. The dashed black line reflects the average of the E_{DB} on an absolute energy scale of -4.60 ± 0.28 eV assuming these band alignments, as described in the text. Note that the DB levels for nitride semiconductors and CdSe were obtained for the zinc-blende phase, while wurtzite was assumed for band alignments.

$(+/-)$ transition levels consistently calculated with the same parameters.[17]

Given the assumed band offsets, the DB levels show reasonable alignment, falling at -5.29 ± 0.24 eV (referenced to the vacuum level) when averaged over the materials in Fig. 3 (the quoted error bar is the standard deviation). This indicates that average DB levels are a reasonable choice for the CNL and could be used to *predict* band offsets. The spread in the other candidates for CNLs such as the E_{BP} level and the H_i $(+/-)$ level is slightly smaller, with E_{BP} falling at -5.19 ± 0.13 eV and the H_i $(+/-)$ level at -4.78 ± 0.15 eV. We note that a significant part of the deviation is due to the values in the II–VI compounds. A similar observation was made in Ref. 16.

We also note that this assessment is sensitive to the assumptions made about the band offsets. For instance, if we use the band alignments reported in Ref. 4 (which were based on explicit calculations for interfaces), we find the results that are plotted in Fig. 4 and also summarized in Table II. This results in values of -4.60 ± 0.28 eV for the average E_{DB} level, -4.44 ± 0.27 eV for the E_{BP}, and -4.03 ± 0.25 eV for the H_i $(+/-)$ level. The upward shift of the averages compared to Fig. 3 [by 0.63 eV for the average DB level, 0.69 eV for E_{BP}, and 0.69 eV for the H_i $(+/-)$ level] is only partly due to the different value assumed for the Si EA (-4.11 eV in Ref. 16 vs -3.68 eV in Ref. 4, a difference of 0.37 eV). The additional upward shift may reflect the fact that the offsets in Ref. 4 were calculated with semilocal functionals, which probably underestimate IPs. However, the spread of the CNL levels around the average is still modest.

All the results confirm the similarity in the DB-derived CNL and the E_{BP} values, which agree within ~ 0.1 eV across all materials, and fall approximately 0.4 eV lower on an absolute scale compared to H_i $(+/-)$.

In Ref. 4, the reason for H_i $(+/-)$ levels acting as a proxy for the CNL was attributed to the fact the H_i in the $+$ charge state strongly binds to an anion, leaving an empty cation DB; H_i in the $-$ charge state strongly binds to a cation, leaving a filled anion DB. The H_i $(+/-)$ level would thus probe the average of the anion and cation DBs, but given the aforementioned occupation of these DBs, the relevant average might be closer to the average of the $(0/-)$ level of the anion DB and the $(+/0)$ level of the cation DB. We find this is the case, with the mean difference falling to -0.44 eV relative to the H_i $(+/-)$ from -0.62 eV as defined relative to the E_{DB} for the full set of materials in Table I. If the Coulomb repulsion U would be identical for anion and cation DBs, then this should produce the same result as the average of the $(+/-)$ levels of the anion and cation DBs that we studied in the present work. However, as noted in Sec. III A, U is larger for anion DBs than for cation DBs. Therefore, the $(0/-)$ level of the anion DB will lie above the $(+/-)$ level by a larger amount than the $(+/0)$ level of the cation DB lies below the corresponding $(+/-)$ level, pushing up the level probed by H_i relative to the average DB level. We suggest this as a (partial) explanation for the fact that the average H_i $(+/-)$ level tracks the average DB level but lies at a higher energy.

IV. CONCLUSIONS

We have performed a systematic study of isolated DBs in group-IV, III–V, and II–VI semiconductors, based on state-of-the-art density functional calculations. We report results for defect levels associated with the various charge states of both cation and anion DBs, and discussed the trends in energy levels and Coulomb repulsion parameter U as a function of lattice constant and atomic size. We also explored whether DB energy levels can define a CNL that can be used to align band structures of semiconductors on an absolute energy scale.

Defining the CNL as E_{DB}, the average value of the $(+/-)$ transition levels for cation- and anion-derived DBs, we indeed find a strong correlation with band alignments obtained from band-offset calculations. We have also compared how this DB-based determination of the CNL compares with other implementations. Strong similarity is found with the branch-point energy, providing a comparably quantitative way to determine band offsets between different semiconductors. We also find that the

alignments are consistent with alignment based on the (+/−) level for interstitial hydrogen,[4] although the hydrogen levels are consistently higher than the DB levels, which we partly attribute to different charge states being probed.

ACKNOWLEDGMENTS

This work was partially performed under the auspices of the U.S. Department of Energy (DOE) by Lawrence Livermore National Laboratory under Contract No. DE-AC52-07NA27344. We also acknowledge support from the Office of Naval Research, Award No.N00014-22-1-2808 (Vannevar Bush Faculty Fellowship). Use was made of computational facilities purchased with funds from the National Science Foundation (No. CNS-1725797) and administered by the Center for Scientific Computing (CSC). The CSC is supported by the California NanoSystems Institute and the Materials Research Science and Engineering Center (MRSEC; NSF DMR) at UC Santa Barbara.

AUTHOR DECLARATIONS

Conflict of Interest

The authors have no conflicts to disclose.

Author Contributions

J. B. Varley: Conceptualization (equal); Data curation (lead); Formal analysis (lead); Writing – original draft (lead); Writing – review & editing (lead). **J. R. Weber:** Conceptualization (equal); Writing – original draft (equal). **A. Janotti:** Conceptualization (equal). **C. G. Van de Walle:** Conceptualization (equal); Writing – review & editing (equal).

DATA AVAILABILITY

The data that support the findings of this study are available from the corresponding author upon reasonable request.

REFERENCES

[1]C. G. Van de Walle and R. A. Street, "Structure, energetics, and dissociation of Si-H bonds at dangling bonds in silicon," Phys. Rev. B **49**, 14766–14769 (1994).
[2]I. Lefebvre, M. Lannoo, C. Priester, G. Allan, and C. Delerue, "Role of dangling bonds at Schottky barriers and semiconductor heterojunctions," Phys. Rev. B **36**, 1336–1339 (1987).
[3]W. Walukiewicz, "Mechanism of Fermi-level stabilization in semiconductors," Phys. Rev. B **37**, 4760–4763 (1988).
[4]C. G. Van de Walle and J. Neugebauer, "Universal alignment of hydrogen levels in semiconductors, insulators and solutions," Nature **423**, 626–628 (2003).
[5]J. Tersoff, "Schottky barrier heights and the continuum of gap states," Phys. Rev. Lett. **52**, 465–468 (1984).
[6]J. Tersoff and W. A. Harrison, "'Pinning' of energy levels of transition-metal impurities," J. Vac. Sci. Technol. B **5**, 1221–1224 (1987).
[7]J. Tersoff and W. A. Harrison, "Transition-metal impurities in semiconductors: Their connection with band lineups and Schottky barriers," Phys. Rev. Lett. **58**, 2367–2370 (1987).
[8]P. W. Peacock and J. Robertson, "Behavior of hydrogen in high dielectric constant oxide gate insulators," Appl. Phys. Lett. **83**, 2025–2027 (2003).
[9]J. E. N. Swallow, R. G. Palgrave, P. A. E. Murgatroyd, A. Regoutz, M. Lorenz, A. Hassa, M. Grundmann, H. V. Wenckstern, J. B. Varley, and T. D. Veal, "Indium gallium oxide alloys: Electronic structure, optical gap, surface space charge, and chemical trends within common-cation semiconductors," ACS Appl. Mater. Interfaces **13**, 2807–2819 (2021).
[10]J. Tersoff, "Calculation of Schottky barrier heights from semiconductor band structures," Surf. Sci. **168**, 275–284 (1986).
[11]C. Tejedor and F. Flores, "A simple approach to heterojunctions," J. Phys. C: Solid State Phys. **11**, L19–L23 (1978).
[12]W. Mönch, "Empirical tight-binding calculation of the branch-point energy of the continuum of interface-induced gap states," J. Appl. Phys. **80**, 5076 (1996).
[13]J. Robertson, "Band offsets, Schottky barrier heights, and their effects on electronic devices," J. Vac. Sci. Technol. A **31**, 050821–050821–18 (2013).
[14]A. Schleife, F. Fuchs, C. Rödl, J. Furthmüller, and F. Bechstedt, "Branch-point energies and band discontinuities of III-nitrides and III-/II-oxides from quasiparticle band-structure calculations," Appl. Phys. Lett. **94**, 012104 (2009).
[15]M. Cardona and N. Christensen, "Acoustic deformation potentials and heterostructure band offsets in semiconductors," Phys. Rev. B **35**, 6182–6194 (1987).
[16]Y. Hinuma, A. Grüneis, G. Kresse, and F. Oba, "Band alignment of semiconductors from density-functional theory and many-body perturbation theory," Phys. Rev. B **90**, 155405 (2014).
[17]J. B. Varley, A. Samanta, and V. Lordi, "Descriptor-based approach for the prediction of cation vacancy formation energies and transition levels," J. Phys. Chem. Lett. **8**, 5059–5063 (2017).
[18]W. Walukiewicz, "Amphoteric native defects in semiconductors," Appl. Phys. Lett. **54**, 2094–2096 (1989).
[19]W. Walukiewicz, "Fermi level dependent native defect formation: Consequences for metal–semiconductor and semiconductor–semiconductor interfaces," J. Vac. Sci. Technol. B **6**, 1257–1262 (1988).
[20]W. Walukiewicz, "Activation of shallow dopants in II–VI compounds," J. Cryst. Growth **159**, 244–247 (1996).
[21]F. Flores and C. Tejedor, "Energy barriers and interface states at heterojunctions," J. Phys. C: Solid State Phys. **12**, 731–749 (1979).
[22]C. Tejedor, F. Flores, and E. Louis, "The metal-semiconductor interface: Si (111) and zincblende (110) junctions," J. Phys. C: Solid State Phys. **10**, 2163–2177 (1977).
[23]P. D. C. King and T. D. Veal, "Conductivity in transparent oxide semiconductors," J. Phys.: Condens. Matter **23**, 334214 (2011).
[24]A. Baldereschi, "Mean-value point in the brillouin zone," Phys. Rev. **B7**, 5212–5215 (1973).
[25]H.-P. Komsa and A. Pasquarello, "Dangling bond charge transition levels in AlAs, GaAs, and InAs," Appl. Phys. Lett. **97**, 191901 (2010).
[26]C. Freysoldt, B. Grabowski, T. Hickel, J. Neugebauer, G. Kresse, A. Janotti, and C. G. Van de Walle, "First-principles calculations for point defects in solids," Rev. Mod. Phys. **86**, 253–305 (2014).
[27]W. Chen and A. Pasquarello, "Accuracy of *GW* for calculating defect energy levels in solids," Phys. Rev. B **96**, 020101 (2017).
[28]P. Broqvist, A. Alkauskas, and A. Pasquarello, "Defect levels of dangling bonds in silicon and germanium through hybrid functionals," Phys. Rev. B **78**, 075203 (2008).
[29]J. R. Weber, A. Janotti, P. Rinke, and C. G. Van de Walle, "Dangling-bond defects and hydrogen passivation in germanium," Appl. Phys. Lett. **91**, 142101 (2007).
[30]J. B. Varley, K. G. Ray, and V. Lordi, "Dangling bonds as possible contributors to charge noise in silicon and silicon-germanium quantum dot qubits," ACS Appl. Mater. Interfaces **15**, 43111–43123 (2023).
[31]B. Shin, J. R. Weber, R. D. Long, P. K. Hurley, C. G. Van de Walle, and P. C. McIntyre, "Origin and passivation of fixed charge in atomic layer deposited aluminum oxide gate insulators on chemically treated InGaAs substrates," Appl. Phys. Lett. **96**, 152908 (2010).
[32]M. Choi, A. Janotti, and C. G. Van de Walle, "Native point defects and dangling bonds in α-Al_2O_3," J. Appl. Phys. **113**, 044501 (2013).
[33]C. Freysoldt, J. Neugebauer, and C. G. Van de Walle, "Fully *ab initio* finite-size corrections for charged-defect supercell calculations," Phys. Rev. Lett. **102**, 016402 (2009); "Electrostatic interactions between charged defects in supercells," Phys. Status Solidi B **248**, 1067–1076 (2010).

[34]J. Heyd, G. E. Scuseria, and M. Ernzerhof, "Hybrid functionals based on a screened Coulomb potential," J. Chem. Phys. **118**, 8207–8215 (2003); "Erratum: Hybrid functionals based on a screened Coulomb potential [J. Chem. Phys.118, 8207 (2003)]," J. Chem. Phys. **124**, 219906 (2006).
[35]P. E. Blöchl, "Projector augmented-wave method," Phys. Rev. B **50**, 17953–17979 (1994).
[36]G. Kresse and J. Furthmüller, "Efficient iterative schemes for ab initio total-energy calculations using a plane-wave basis set," Phys. Rev. B **54**, 11169–11186 (1996); "Efficiency of ab-initio total energy calculations for metals and semiconductors using a plane-wave basis set," Comp. Mater. Sci. **6**, 15–50 (1996).
[37]J. Paier, M. Marsman, K. Hummer, G. Kresse, I. C. Gerber, and J. G. Ángyán, "Screened hybrid density functionals applied to solids," J. Chem. Phys. **124**, 154709 (2006).
[38]O. Madelung, *Semiconductors: Data Handbook* (Springer Verlag, 2004).
[39]J. Tersoff, "Schottky barriers and semiconductor band structures," Phys. Rev. B **32**, 6968–6971 (1985).
[40]P. W. Anderson, "Model for the electronic structure of amorphous semiconductors," Phys. Rev. Lett. **34**, 953–955 (1975).
[41]Y. K. Frodason, C. Zimmermann, E. F. Verhoeven, P. M. Weiser, L. Vines, and J. B. Varley, "Multistability of isolated and hydrogenated Ga-O divacancies in β-Ga_2O_3," Phys. Rev. Mater. **5**, 025402 (2021).
[42]C. Linderalv, A. Lindman, and P. Erhart, "A unifying perspective on oxygen vacancies in wide band gap oxides," J. Phys. Chem. Lett. **9**, 222–228 (2018).
[43]D. J. Chadi and K. J. Chang, "Theory of the atomic and electronic structure of DX centers in GaAs and $Al_xGa_{1-x}As$ alloys," Phys. Rev. Lett. **61**, 873–876 (1988).
[44]L. Gordon, J. L. Lyons, A. Janotti, and C. G. Van de Walle, "Hybrid functional calculations of DX centers in AlN and GaN," Phys. Rev. B **89**, 085204 (2014).
[45]S. Mu, M. Wang, J. B. Varley, J. L. Lyons, D. Wickramaratne, and C. G. Van de Walle, "Role of carbon and hydrogen in limiting n-type doping of monoclinic $(Al_xGa_{1-x})_2O_3$," Phys. Rev. B **105**, 155201 (2022). 2111.07194.
[46]D. Wickramaratne, J. B. Varley, and J. L. Lyons, "Donor doping of corundum $(Al_xGa_{1-x})_2O_3$," Appl. Phys. Lett. **121**, 042110 (2022).
[47]B. Cordero, V. Gómez, A. E. Platero-Prats, M. Revés, J. Echeverría, E. Cremades, F. Barragán, and S. Alvarez, "Covalent radii revisited," Dalton Trans. **2008**, 2832–2838.
[48]E. A. Davis, S. F. J. Cox, R. L. Lichti, and C. G. Van de Walle, "Shallow donor state of hydrogen in indium nitride," Appl. Phys. Lett. **82**, 592–594 (2003).
[49]J. Shin, G. A. Gamage, Z. Ding, K. Chen, F. Tian, X. Qian, J. Zhou, H. Lee, J. Zhou, L. Shi, T. Nguyen, F. Han, M. Li, D. Broido, A. Schmidt, Z. Ren, and G. Chen, "High ambipolar mobility in cubic boron arsenide," Science **377**, 437–440 (2022).
[50]K. Bushick, S. Chae, Z. Deng, J. T. Heron, and E. Kioupakis, "Boron arsenide heterostructures: Lattice-matched heterointerfaces and strain effects on band alignments and mobility," npj Computat. Mater. **6**, 3 (2020).
[51]J. L. Lyons, J. B. Varley, E. R. Glaser, J. A. Freitas, J. C. Culbertson, F. Tian, G. A. Gamage, H. Sun, H. Ziyaee, and Z. Ren, "Impurity-derived p-type conductivity in cubic boron arsenide," Appl. Phys. Lett. **113**, 251902 (2018).
[52]G. Brammertz, H. Lin, K. Martens, A.-R. Alian, C. Merckling, J. Penaud, D. Kohen, W.-E. Wang, S. Sioncke, A. Delabie, M. Meuris, M. R. Caymax, and M. Heyns, "Electrical properties of III-V/oxide interfaces," ECS Trans. **19**, 375–386 (2009).